

Electronic Supporting Information

Elucidating the endocytosis, intracellular trafficking, and exocytosis of carbon dots in neural cells

Nan Zhou,^a Shoujun Zhu,^b Suraj Maharjan,^a Zeyu Hao,^a Yubin Song,^b Xiaohuan Zhao,^b Yanfang Jiang,^c Bai Yang^{*b} and Laijin Lu^{*a}

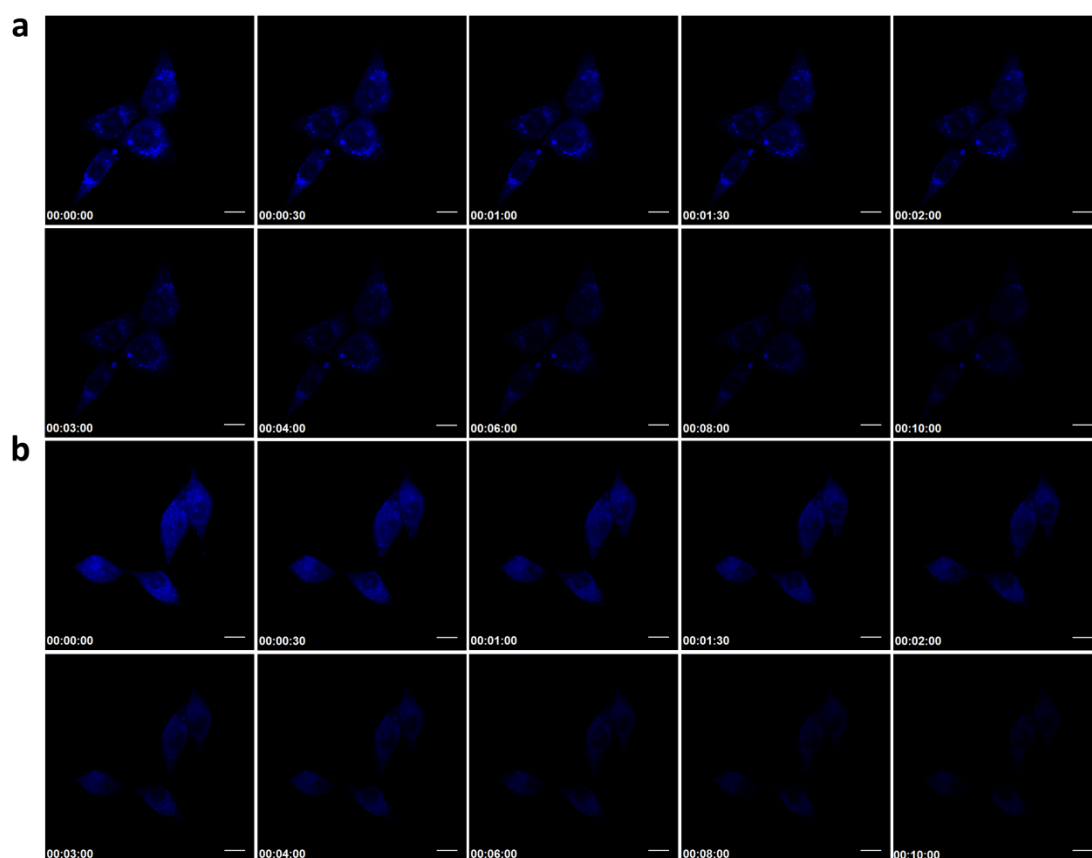


Fig. S1. Photostability of CDs in PC12 (a) and RSC96 (b) cells.

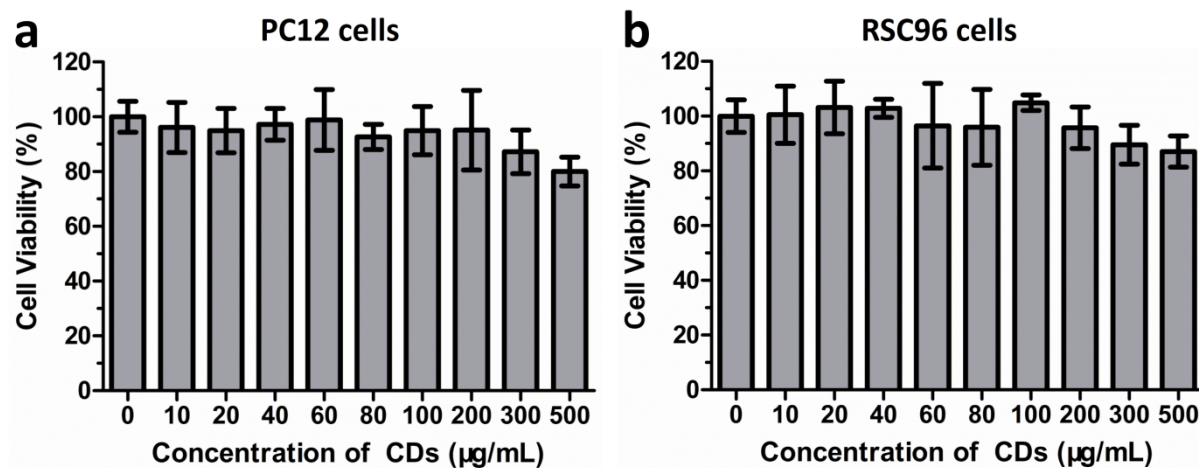


Fig. S2. Low cytotoxicity of CDs in PC12 (a) and RSC96 (b) cells. The values are expressed as mean \pm SD (n = 6).

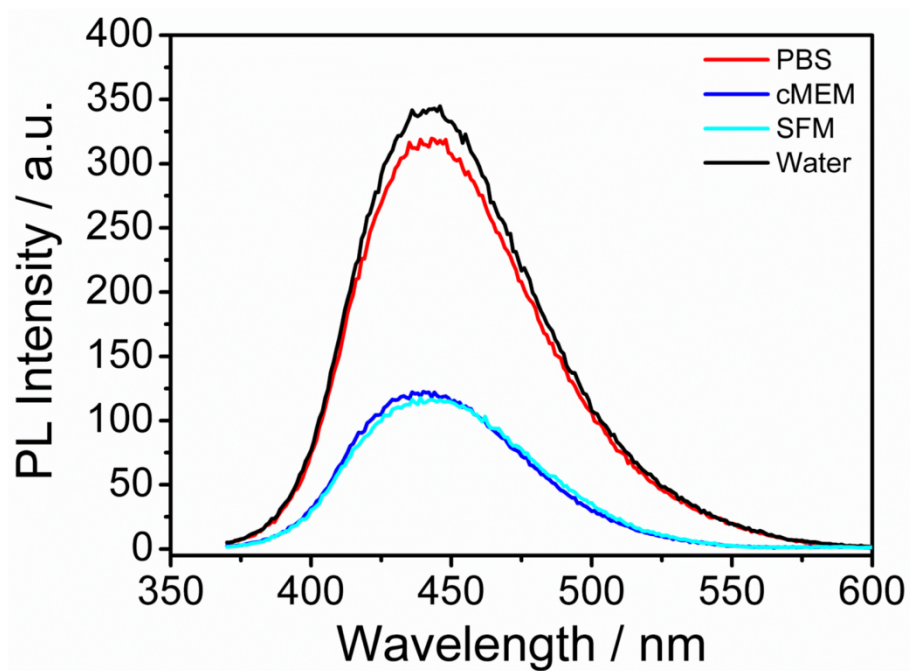


Fig. S3. Fluorescence quenching of CDs in the presence of culture media and no obvious difference of PL intensity of CDs between cMEM and SFM. PBS: phosphate buffer solution; cMEM: complete culture media (10% fetal bovine serum added); SFM: serum free media.

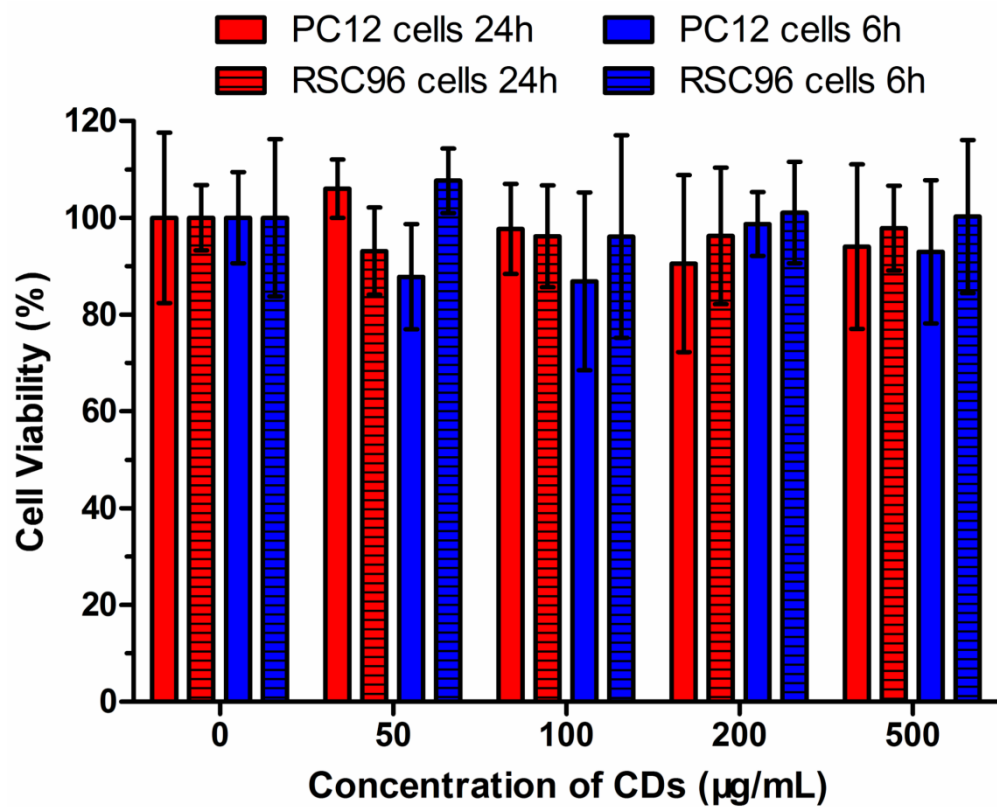


Fig. S4. No significant cytotoxicity of CDs is observed in serum free media during 24h or 6h. The values are expressed as mean \pm SD (n = 3).

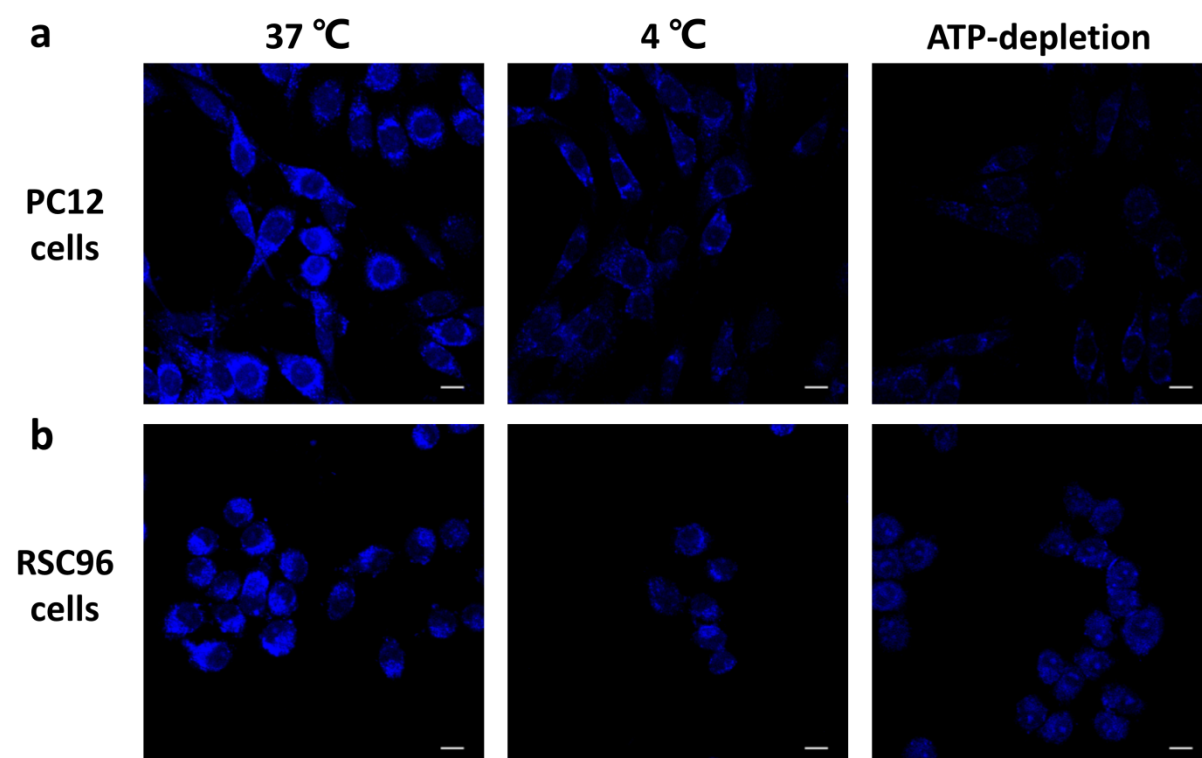


Fig. S5. CLSM images of cellular uptake of CDs after 45 min incubation with CDs at 37 °C, 4 °C and ATP-depletion treatments (The scale bar is 10 μ m).

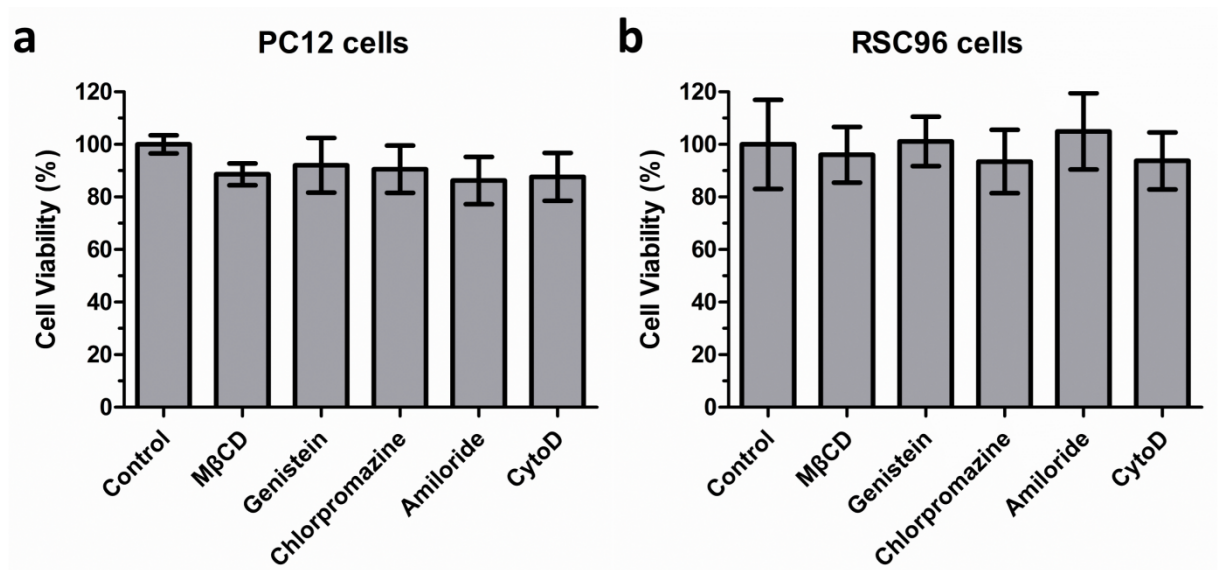


Fig. S6. No significant cytotoxicity of cellular uptake inhibitors is observed after 4 h incubation. M β CD (2 mM, methyl- β -cyclodextran), genistein (50 μ g/mL), chlorpromazine (10 μ g/mL), amiloride (50 μ M) and CytoD (5 μ M, cytochalasin D). The values are expressed as mean \pm SD (n = 3).

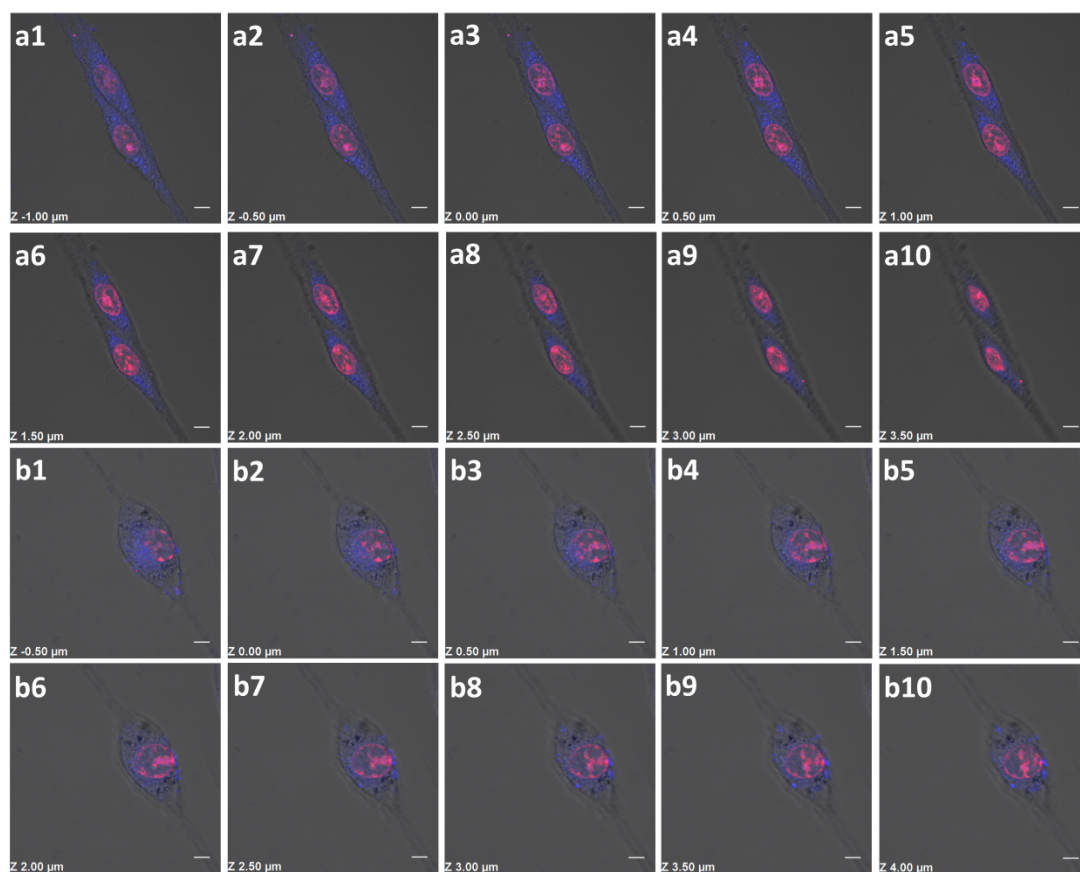


Fig. S7. XYZ scan images of PC12 (a) and RSC96 (b) cells incubated with CDs and propidium iodide (a red fluorescent nuclear dye). Z step is 0.5 μm and scale bar is 5 μm .

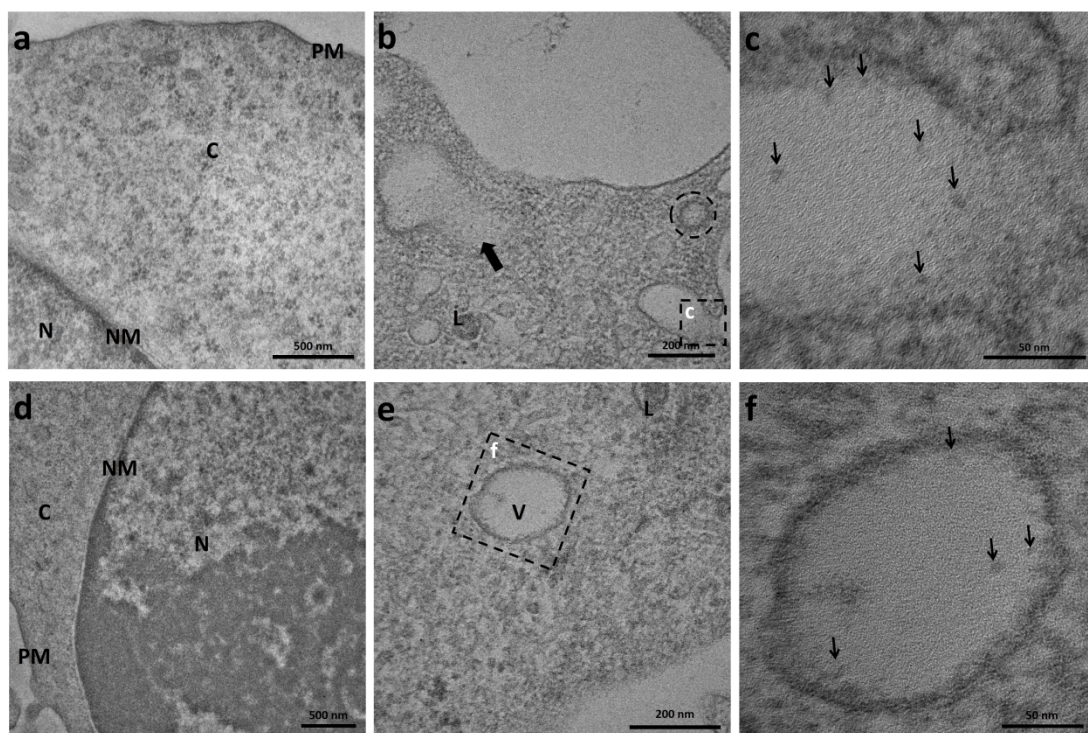


Fig. S8. Endocytosis and intracellular distribution of CDs were observed by TEM in PC12 (a-c) and RSC96 (d-f) cells. Plasma membrane (PM), cytoplasm (C), nuclear membrane (NM) and nucleus (N) of untreated PC12 (a) and RSC96 (d) cells were observed. Cells were incubated with CDs for 1 h (b and e). (b) Large accumulation of CDs were inside the cell indicated by thick arrows and were also observed in the invagination structures of cell membrane enlarged in (c). The dotted circle showed a clathrin-coated pit. Lysosomes (L) had higher contrast resulting in difficultly distinguishing CDs. (e) An endocytic vesicle (V) was found inside the cells and magnified in (f). In the view field of 200,000 X (c) and 150,000 X (f), we found some medium electron-dense contrast particles with the size of 3-8 nm which were similar with CDs (thin arrows), compared with the low contrast cell background.

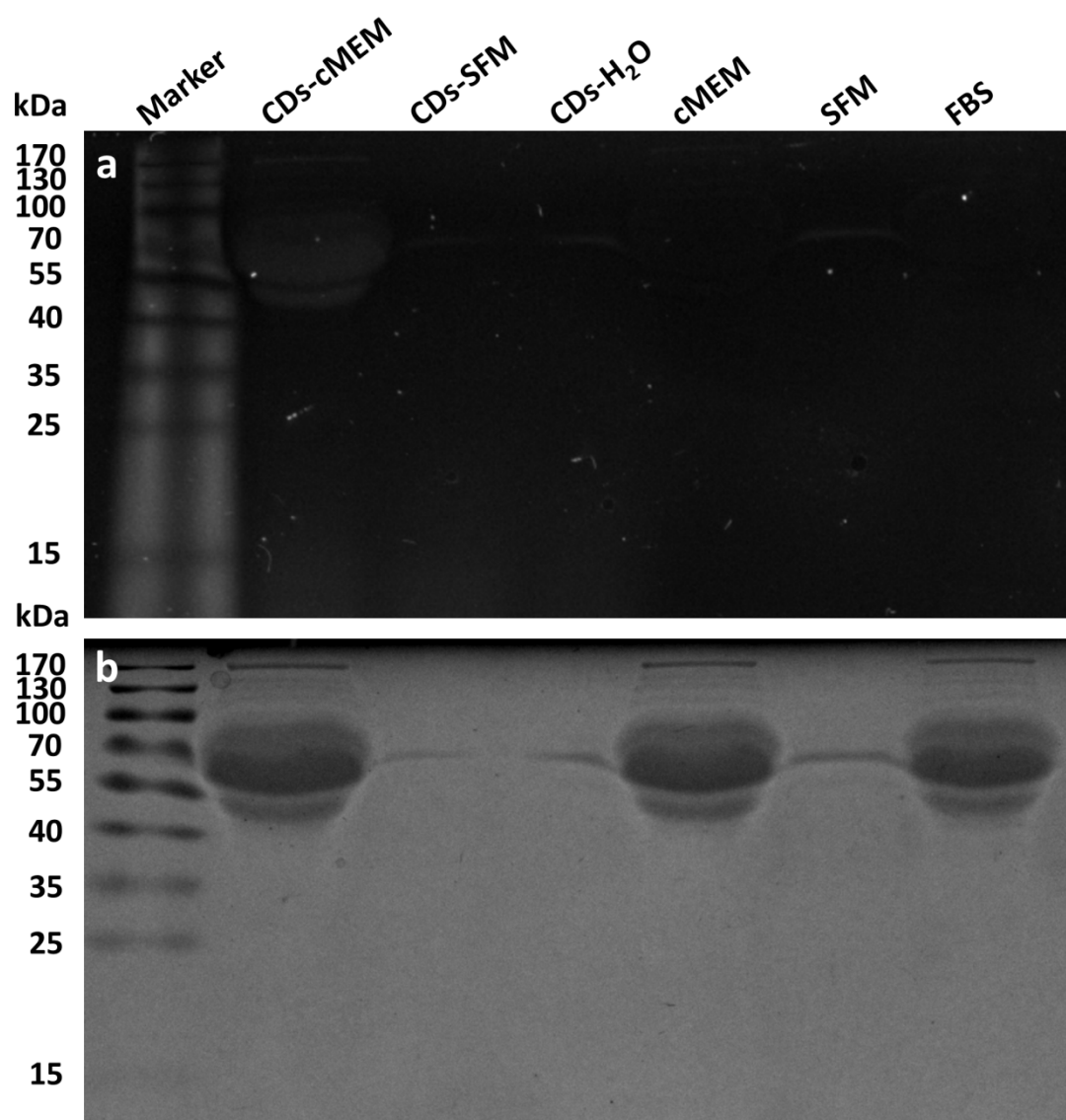


Fig. S9. CDs exposed to serum proteins formed a protein-CDs complex by observing at UV light (a) and Coomassie Blue staining (b).

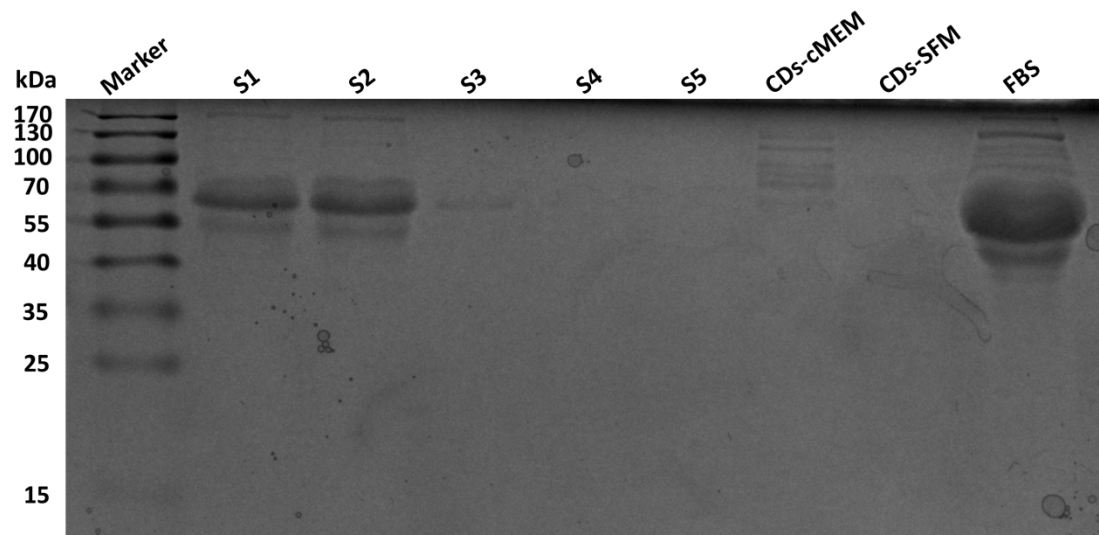


Fig. S10. The formation of hard corona proteins on the surface of CDs. CDs were incubated with cMEM (CDs-cMEM) at 37 °C for 2 h. SDS-PAGE of supernatants (S) were following repeated centrifugation (18,000 *g* for 20 min) and wash steps of CDs. S1 was diluted by a factor of 10 to avoid overloading the gel. After five centrifugation-wash steps (S5), protein was no longer visible in the supernatant and the pellet containing high-affinity, tightly bound (hard corona) proteins was collected. Moreover, CDs incubated with SFM (CDs-SFM) at 37 °C for 2 h was used for comparison. All samples were incubated for 5 min at 100 °C to denature the proteins, cooled to room temperature and finally loaded onto a polyacrylamide gel for electrophoresis. Coomassie Blue stained gel showed that the corona proteins were divided in some groups by their molecular weight (55-70, 70-100, and 100-130 kDa).

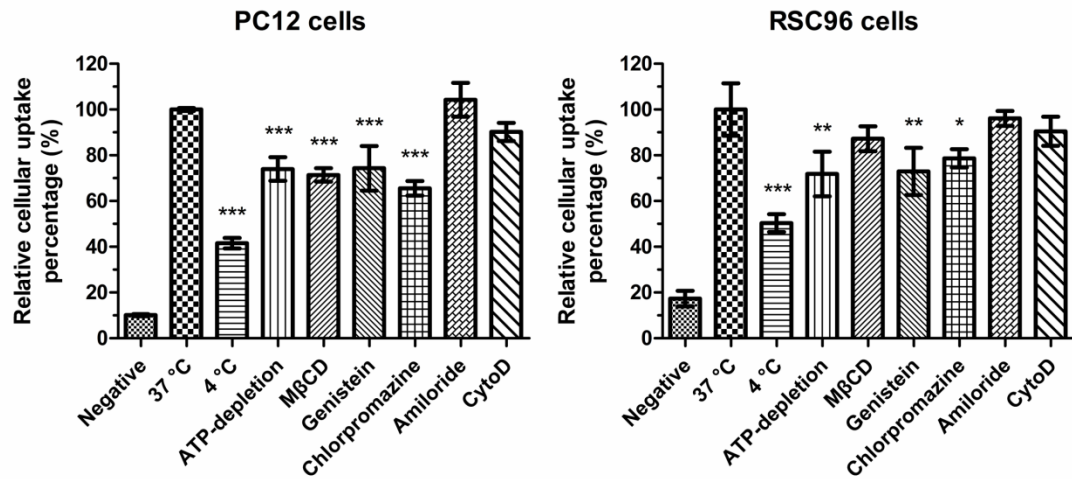


Fig. S11. Quantitative analysis of influence of uptake inhibitors for cellular uptake pathways in cMEM. MβCD: methyl-β-cyclodextran; CytoD: cytochalasin D. The values are expressed as mean ± SD (n = 3). * $P < 0.05$, ** $P < 0.01$, *** $P < 0.001$, compared with 37 °C group, using one-way ANOVA.

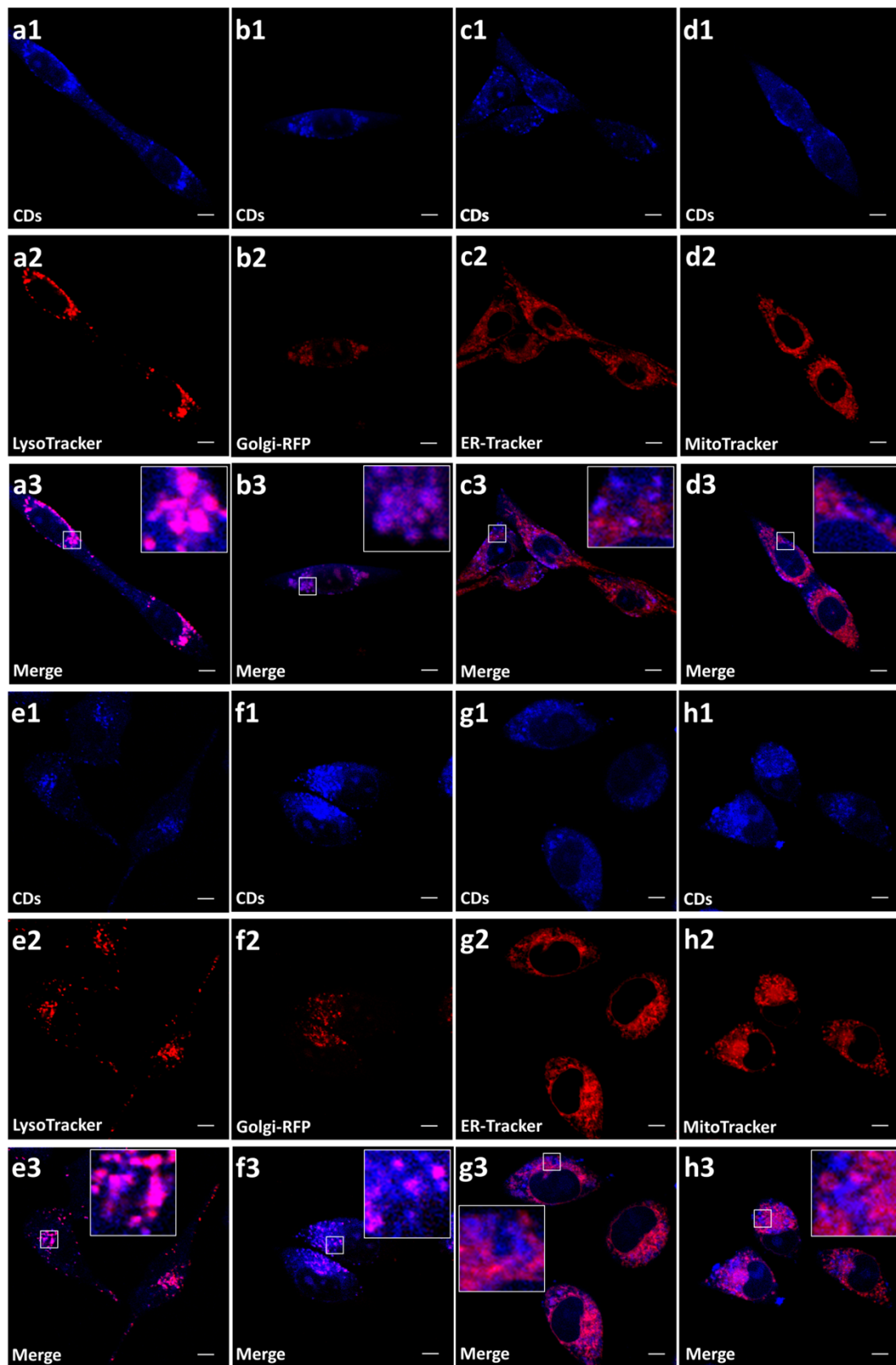


Fig. S12. Intracellular distribution of CDs in PC12 and RSC96 cells within cMEM. Pink spots in the merged images indicate colocalization of CDs and lysosomes along with Golgi apparatus. The scale bar is 5 μ m and representative areas are magnified optically.

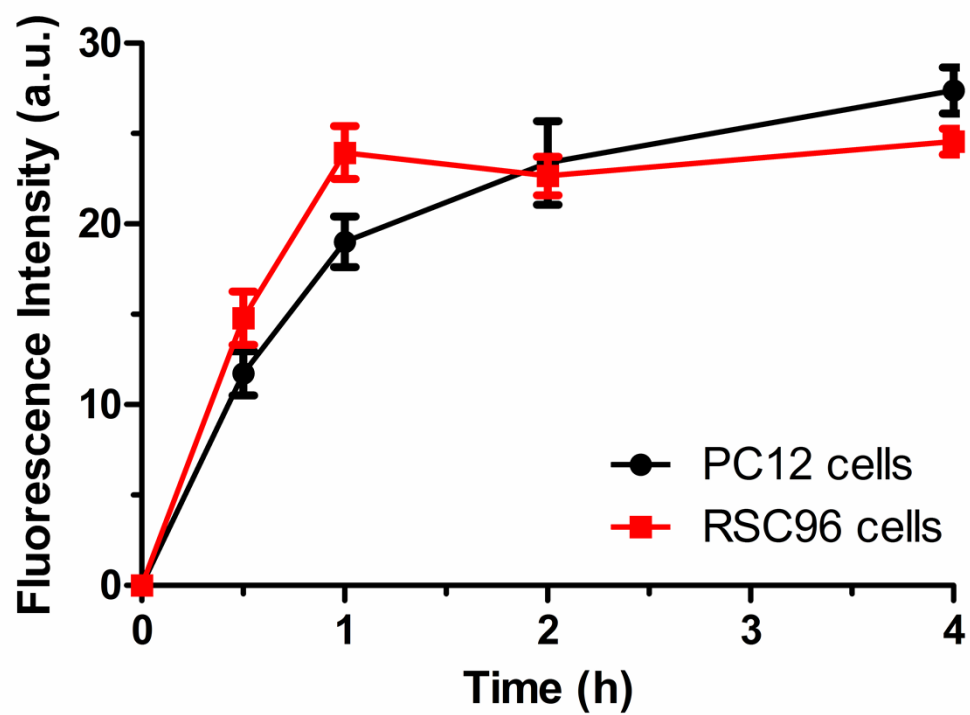


Fig. S13. Fluorescence intensity of CDs exocytosed into the medium from the cells at different time points. The values are expressed as mean \pm SD ($n = 3$).

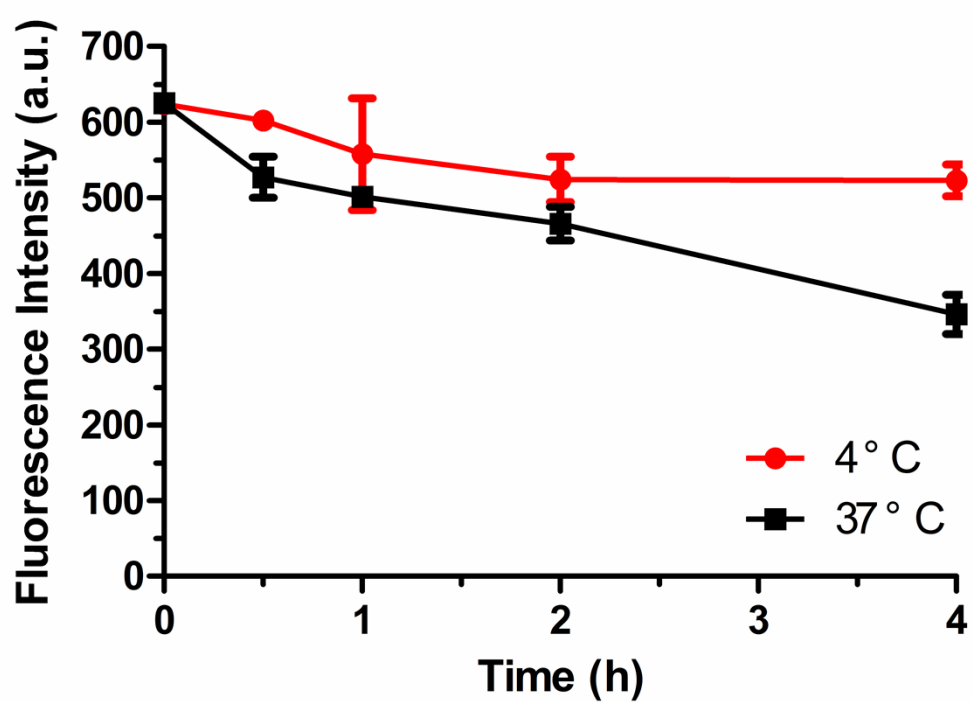


Fig. S14. FACS analysis of the exocytosis of CDs at 4 °C and 37 °C in RSC96 cells. The values are expressed as mean \pm SD (n = 3).

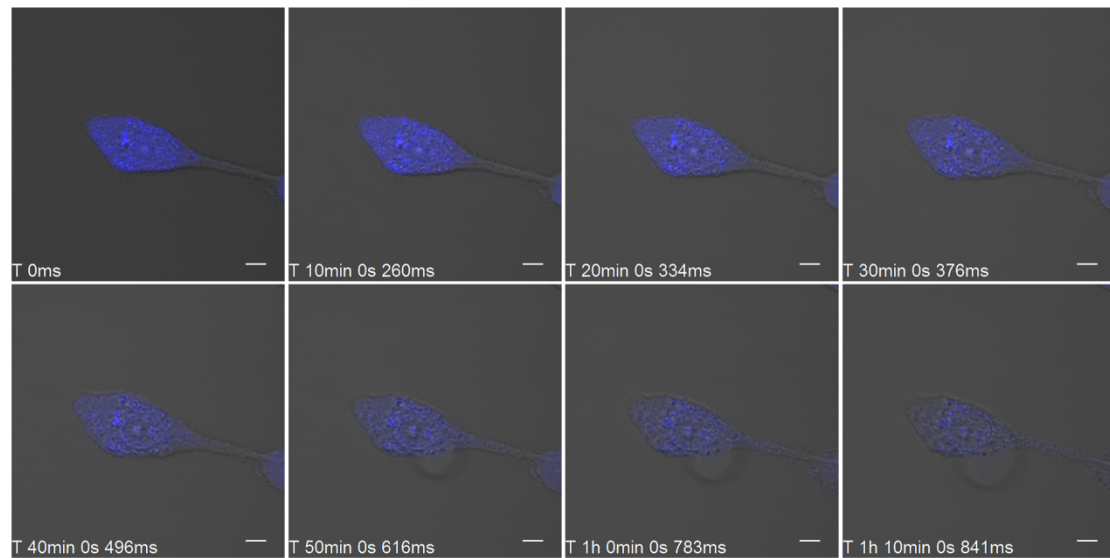


Fig. S15. Exocytosis of CDs was observed by time-lapse imaging in RSC96 cells. The scale bar is 5 μm .

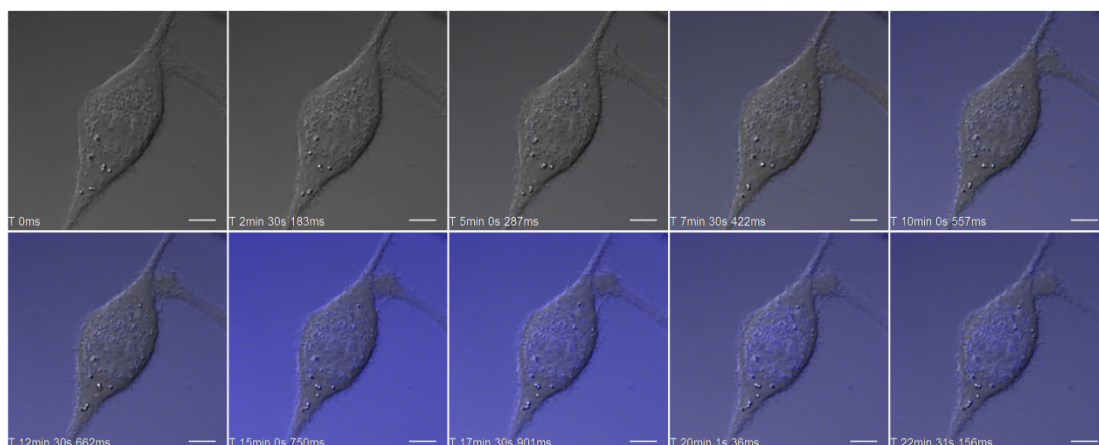


Fig. S16 Dynamic confocal imaging of endocytosis of CDs in RSC96 cells. The scale bar is 5 μm .

References:

1. A. Lesniak, F. Fenaroli, M.P. Monopoli, C. Aberg, K.A. Dawson and A. Salvati, *ACS Nano*, 2012, **6**, 5845.
2. C.C. Fleischer and C.K. Payne, *J. Phys. Chem. B*, 2012, **116**, 8901.
3. T. Cedervall, I. Lynch, M. Foy, T. Berggård, S.C. Donnelly, G. Cagney, S. Linse and K.A. Dawson, *Angew. Chem. Int. Ed. Engl.*, 2007, **46**, 5754.
4. M.P. Monopoli, D. Walczyk, A. Campbell, G. Elia, I. Lynch, F.B. Bombelli and K.A. Dawson, *J. Am. Chem. Soc.* 2011, **133**, 2525.
5. C.C. Fleischer, U. Kumar and C.K. Payne, *Biomater. Sci.*, 2013, **1**, 975.